ISSN 1063-7850, Technical Physics Letters, 2016, Vol. 42, No. 3, pp. 243–247. © Pleiades Publishing, Ltd., 2016.
Original Russian Text © M.N. Drozdov, Yu.N. Drozdov, A.V. Novikov, P.A. Yunin, D.V. Yurasov, 2016, published in Pis'ma v Zhurnal Tekhnicheskoi Fiziki, 2016, Vol. 42, No. 5, pp. 40–48.

# Nonlinear Calibration Curves in Secondary Ion Mass Spectrometry for Quantitative Analysis of GeSi Heterostructures with Nanoclusters

**M. N. Drozdov[a, b]*, Yu. N. Drozdov[a, b], A. V. Novikov[a, b], P. A. Yunin[a, b], and D. V. Yurasov[a, b]**

[a] *Institute for Physics of Microstructures, Russian Academy of Sciences, Nizhny Novgorod, 603950 Russia*
[b] *Lobachevsky State University of Nizhny Novgorod, Nizhny Novgorod, 603950 Russia*
**e-mail: drm@ipm.sci-nnov.ru*

Received September 25, 2015

**Abstract**—For the first time in the practice of secondary ion mass spectrometry, we obtained a nonlinear calibration curve for the ratio of the cluster and elementary secondary ions of germanium $Ge_2/Ge$ without secondary ions of silicon, which enables the quantification of germanium in $Ge_xSi_{1-x}$ heterostructures in the entire range of $0 < x \leqslant 1$. We developed a method for quantitative lateral analysis based on the plotting of a lateral map of $x$. An algorithm to identify and analyze the lateral heterogeneity of $x$ in $Ge_xSi_{1-x}$ heterostructures with 3D clusters by comparing the results of depth profiling analysis, obtained using linear and nonlinear calibration curves, is developed, and concentration $x$ in the self-assembled nanoislands is determined.

**DOI:** 10.1134/S1063785016030044

The most common approach to quantitative analysis of the elemental composition of semiconductor heterostructures by secondary ion mass spectrometry (SIMS) is the search for linear calibration ratios that can compensate nonlinear matrix effects. The availability of linear calibration curves of the intensity of secondary ions (more precisely, some combination of secondary ions) on concentration offers a very simple and convenient procedure for processing experimental results to determine the concentration profiles of elements and significantly decreases the number of necessary test structures. The best known is the $CsM^+$ approach, in which positive cluster ions of element M of the matrix are recorded after sputtering by cesium ions [1–5]. For $Ge_xSi_{1-x}$ heterostructures, a linear calibration curve for elementary secondary ions was also found [2, 5–7],

$$\mathrm{Ge/Si} = K_1 x/(1-x). \quad (1)$$

We found in recent studies [5, 8] that, for $Ge_xSi_{1-x}$ heterostructures, along with linear dependences, there is a nonlinear relationship for cluster secondary $Ge_2$ ions. In the range of $0 < x < 0.4$, the following quadratic dependence is true for the ratio of $Ge_2/Si$:

$$\mathrm{Ge_2/Si} = K_2(x/(1-x))^2. \quad (2)$$

Equations (1) and (2) suggested another option of nonlinear calibration, that is,

$$\mathrm{Ge_2/Ge} = K_3 x/(1-x), \quad (3)$$

where $K_3 = K_2/K_1$, which was also found in [5, 8]. Dependences (2) and (3) are clearly associated with a rather strong manifestation of matrix effects. Only this can explain the fact that the intensity of silicon secondary ions is not included at all in Eq. (3), and concentration $x$ may be searched using two different secondary ions of germanium. Previously, we have not seen the use of such dependences in the practice of SIMS.

For $Ge_xSi_{1-x}$ heterostructures with planar layers, calibration equations (2) and (3) give concentration profiles of $x$ coinciding with that obtained using Eq. (1) and differ only in a lower dynamic range of $x$ [5]. Therefore, the original nonlinear calibration mode seemed something exotic. At the same time, it was experimentally found that for $Ge_xSi_{1-x}$ heterostructures with 3D nanoclusters, the linear and nonlinear calibrations gave completely different profiles of $x$, and a qualitative explanation of this fact was proposed [8]. In [8], heterostructures with self-assembled $Ge_xSi_{1-x}$ nanoislands were studied for which the size of analyzed 3D objects in the plane of growth was much smaller than the diameter of a probe ion beam. In this case, germanium secondary ions appearing in linear equation (1) only occur in regions of nanoislands or wetting layers, while the signal of silicon secondary ions emerges from both the islands and the surrounding regions of pure silicon. This results in a significant underestimation of concentration $x$ determined by linear calibration equation (1). At the same time, all the measured secondary ions in Eq. (3) are determined only by the regions containing germanium. We can therefore expect that, according to Eq. (3), concentration $x$ will always be close to the real

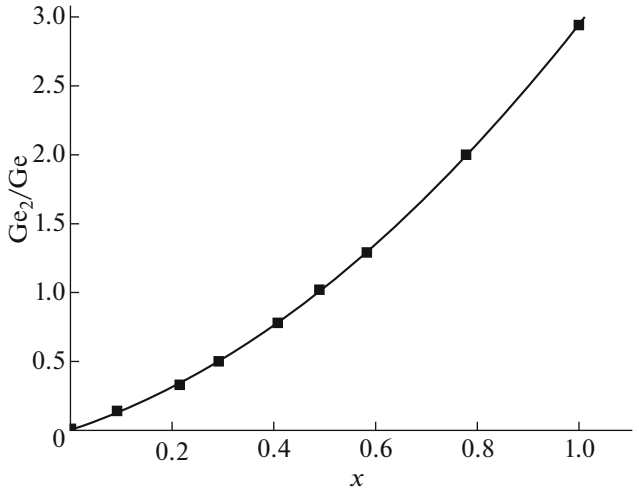


**Fig. 1.** Dependence of the ratio of the intensities of $Ge_2/Ge$ secondary ions on germanium concentration $x$ (squares) obtained with the use of test structures and (solid line) approximating an analytical curve (Eq. (4)).

concentration in nanoislands. We have demonstrated in [8] that it is possible to distinguish between planar layers and layers with 3D nanoislands and to estimate the height of the islets, the presence of a wetting layer, etc., from SIMS measurements using Eqs. (1) and (3) without additional a priori information about the structure. This gives more information about the multilayer heterostructures with clusters in the depth profiling analysis by SIMS.

However, nonlinear calibration equations (2) and (3) derived in [5, 8] were limited by a narrow concentration region of $0 < x < 0.4$, which left the question of whether such an approach is universal for structures with arbitrary $x$. The reason for the differences between the value of $x$ measured in nanoislands ($x$ = 0.22–0.25) and the real value of $x$, which was approximately 0.4 for the mode of islet growth used in [8], also remained unclear. The goal of the present Letter is to clarify these issues. A new calibration equation will be obtained experimentally for the ratio of secondary ions of $Ge_2/Ge$ for the entire range of $0 < x \leqslant 1$. In order to determine the actual concentration $x$ in nanoislands, a method for the quantitative lateral analysis of $x$ distribution—lateral mapping of $x$—will be developed using the above equation.

We used a TOF.SIMS-5 secondary ion mass spectrometer in this study to analyze the semiconductor structures. Probing was conducted by bismuth ions with an energy of 25 keV and a beam current of 1 pA scanning in a raster of 128 × 128 pixels. Each pixel corresponded to one pulse of bismuth ions. Sputtering was performed by cesium ions with an energy of 1 keV and a beam current of 50 nA. Two structures of $Ge_xSi_{1-x}$/Si, A and B, were used for the quantitative calibration; each structure consisted of three $Ge_xSi_{1-x}$ layers 200 nm in thickness with different concentrations of $x$: 0.09–0.29–0.47 for Structure A and 0.21–0.41–0.58 for Structure B [5, 8]. Structure C with a layer of $Ge_{0.78}Si_{0.22}$ 500 nm in thickness grown on a substrate of germanium Ge(001) was additionally used for the calibration, which made it possible to expand the calibration range up to $x = 1$. To demonstrate the possibility of the quantitative analysis of the lateral distribution of germanium, we investigated Structure D, which included 20 layers of Ge(Si) self-assembled islands, separated by layers of silicon. This structure specifically was analyzed in our study [8].

Figure 1 shows the dependence of the ratio of secondary ions $Ge_2/Ge$ on germanium concentration $x$; it is approximated by an analytical curve, a second-order polynomial, that is,

$$Ge_2/Ge = 1.206x + 1.735x^2. \quad (4)$$

In contrast to [5, 8], where only the main isotopes of germanium $^{74}Ge$ and $^{126}Ge_2$ were used, in this study, we operated the sum of all isotopes of Ge and $Ge_2$, which enhanced the intensity of the secondary ions by three to four times. This was especially important for the regions of low concentrations of germanium. The result is a rather high degree of correlation of the experimental data and the approximating polynomial; the correlation coefficient is $R = 0.99993$. The accuracy achieved by almost two orders of magnitude greater than the accuracy of Eq. (3) in [8]. Using Eq. (4), concentration $x$ can be determined analytically from the results of measurements of the intensity of secondary Ge and $Ge_2$ ions throughout the entire range of $0 < x \leqslant 1$.

The profiles of $x$ for the first two layers of the surface of nanoislands in Structure D obtained by calibration equations (1) and (4) are presented in Fig. 2. It is seen from Fig. 2a that concentration $x$ at the maximum of the profile determined by nonlinear calibration equation (4) significantly exceeds the results obtained by the linear calibration. At the same time, as already mentioned, the maximum value of concentration $x \sim 0.22$ determined from the nonlinear calibration curve is lower than the actual concentration in the islands, which amounts to $x \sim 0.4$. In our opinion, the reason for this discrepancy is as follows. In plotting a depth profile of $x$ by Eq. (4), the intensity of $Ge_2$ and Ge secondary ions from all regions containing germanium, such as islands of wetting layers and individual clusters and regions of $Ge_xSi_{1-x}$ formed either during growth of the multilayer structure or as artifacts of the depth profiling are summed in a raster of probe bismuth ions. Therefore, the profile of $x$ reflects the integrated concentration in all regions containing germanium; complete information on concentration $x$ in some areas can only be obtained from the lateral map of $x$ distribution in the layer of nanoislands.

In this study, a new approach to plotting a quantitative lateral map of germanium concentration is

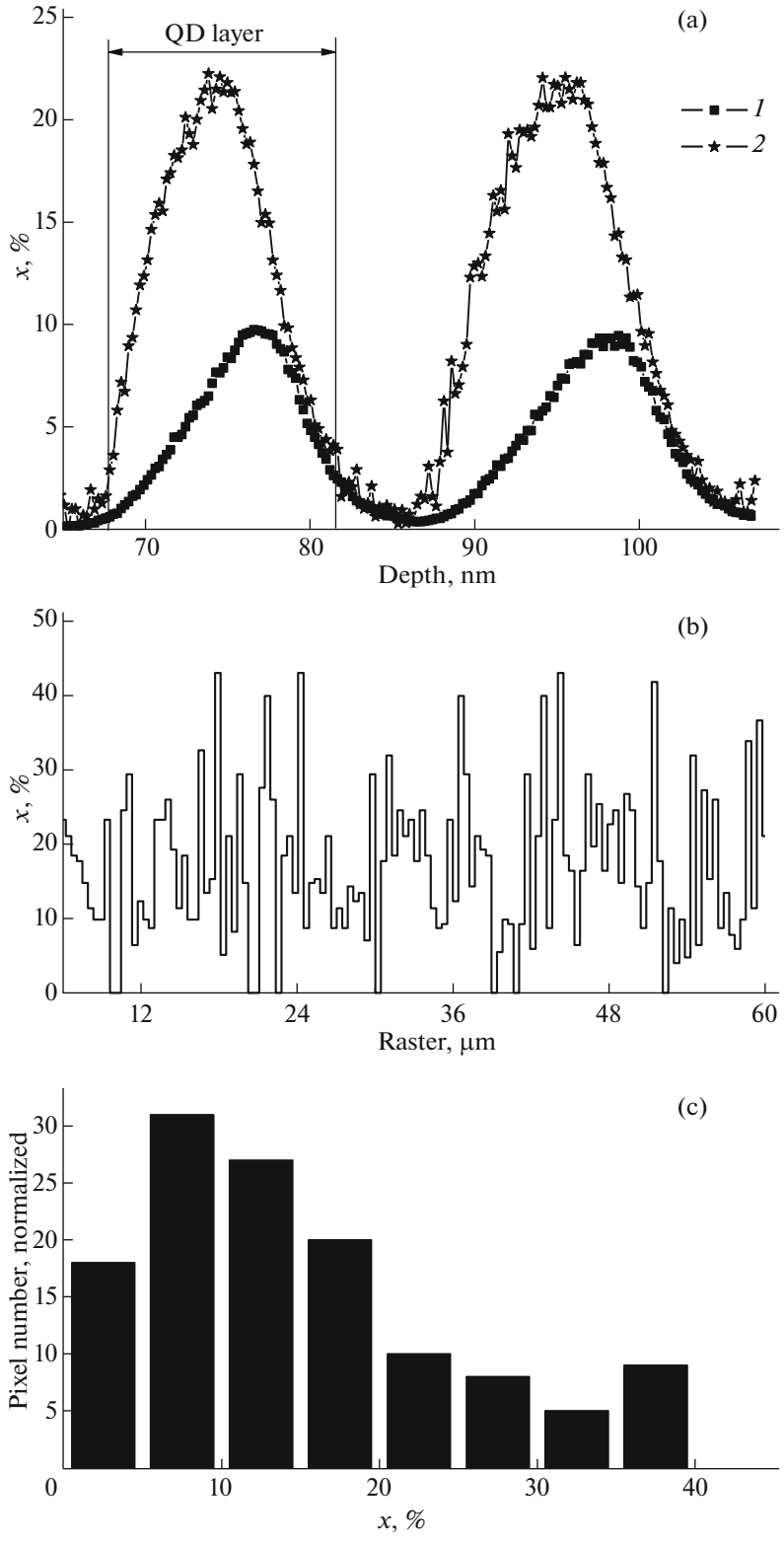


**Fig. 2.** (a) Concentration profile of germanium in the first two layers of the surface of nanoislands in Structure D obtained using two different calibration curves: (*1*) linear dependence of Ge/Si and (*2*) nonlinear dependence of $Ge_2$/Ge; vertical lines show the region of nanoislands, quantum dots. (b) Lateral distribution of concentration $x$ for nonlinear calibration curve (Eq. (4)) in one of the horizontal sections of the raster. (c) Histogram of the distribution of concentration $x$ for the nonlinear calibration curve over the pixels of lateral raster.

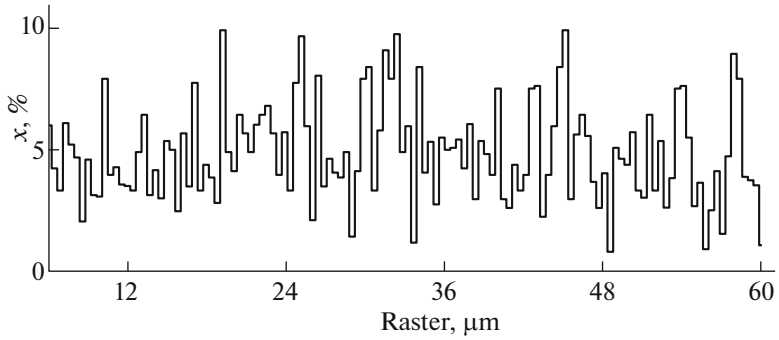


**Fig. 3.** Lateral distribution of concentration $x$ for the linear calibration curve in one of the horizontal sections of the raster.

developed. All the necessary experimental data contained in the files of depth profiling of the TOF.SIMS-5 instrument, including a full mass spectrum of each of the 128 × 128 pixels for each of the rasters of the probe beam for the full time of analysis. The intensity of Ge and $Ge_2$ secondary ions in one pixel is small; therefore, the lateral images of several tens of rasters were summed so that the signal was at least ten times greater than noise. In this way, we obtained the lateral images of secondary ions of Si, Ge, and $Ge_2$, including all isotopes used for calibration in Eqs. (1) and (4). These images were exported from the TOF.SIMS-5 program as *.txt files; the lateral image of concentration $x$ in the raster of probe bismuth ions was plotted based on these data. One of the horizontal sections of this image is shown in Fig. 2b, and Fig. 2c shows a histogram of concentration $x$ distributions over the number of pixels of the raster. The image was obtained for the layer of nanoislands, marked in Fig. 2a by vertical lines. As follows from Fig. 2b, the range of changes in the germanium concentration in the growth plane is from 0 to 0.43. In the histogram in Fig. 2c, there are two peaks: in the region of $x \sim 0.4$ and near $x \sim 0.1$. It is natural to assume $x = 0.43$ to be the concentration of germanium in the islands, that is, the regions with its highest concentration on the surface. Average concentration $x$ in nanoislands is, as shown in Fig. 2c, $x \sim 0.4$. The second maximum of $x \sim 0.1$, apparently, corresponds to the germanium concentration measured in a thin wetting layer. This value, in our view, is below the real concentration, because the depth resolution (2–3 nm) is insufficient for analysis of the wetting layer with a thickness of less than 1 nm [8, 9], and, at this time, the concentration cannot be measured more accurately. It is noteworthy that the lateral map of $x$ is of rather rugged nature, with sharp changes from zero to maximum (Fig. 2b). This is definitely related to the ratio of the lateral scales of nanoislands (0.1–0.15 μm) and the diameter of the beam of probing bismuth ions (2–3 μm). Therefore, the characteristic lateral scale of the resulting map of $x$ is consistent with one pixel in the raster of bismuth ions rather than determined by the actual size of nanoislands.

The lateral map of $x$ obtained using a linear calibration relationship (Fig. 3) gives a completely different low result: the value of $x$ varies from 0.01 to 0.1, while the average value of $x$ is approximately 0.04. It is clear that the reason for this difference from the result obtained by the nonlinear calibration dependence is the same as already discussed for the profile of $x$.

Thus, we obtained for the first time a nonlinear calibration curve for the ratio of the cluster and elementary secondary ions of germanium $Ge_2/Ge$, without secondary ions of silicon, which enables quantification of germanium in $Ge_xSi_{1-x}$ heterostructures in the entire range of $0 < x \leqslant 1$. The algorithm for identifying and analyzing the lateral heterogeneity of $x$ in $Ge_xSi_{1-x}$ heterostructures with 3D clusters by comparing the results of depth profiling obtained using linear and nonlinear calibration curves obtained earlier in [8] is developed. The linear calibration curve includes the normalization for silicon secondary ions and significantly understates the concentration of germanium in nanoislands. The depth profiling using the ratio of $Ge_2/Ge$ gives a much more accurate result for $x$ in nanoislands, because it involves secondary ions only from the areas containing germanium. The method of quantitative lateral analysis of the map of $x$ proposed in this work gives an even more detailed information on laterally inhomogeneous structures. For heterostructures with nanoislands, the most important statistical characteristics of arrays of nanoislands can be found, such as a characteristic concentration $x$ in the islands and the presence of additional maxima in the histogram of $x$ distribution over the pixels, associated with the wetting layer.

**Acknowledgments.** This work was supported by the Russian Foundation for Basic Research (project no. 15-02-02947) and the Ministry of Education and Science of the Russian Federation according to agreement between the Ministry of Education and Science and Lobachevskii State University, Nizhny Novgorod, no. 02.V.49.21.0003 of August 27, 2013. The equipment of the Common Use Center of Institute for Physics of Microstructures, Russian Academy of Sciences, was used in the study.

## REFERENCES

1. Y. Gao, J. Appl. Phys. **67**, 3760 (1988).
2. B. Gautier, J. C. Dupuy, and C. Dubois, Thin Solid Films **294**, 54 (1997).
3. M. Gavelle, E. Scheid, F. Cristiano, et al., J. Appl. Phys. **102**, 074904 (2007).
4. M. N. Drozdov, Yu. N. Drozdov, D. N. Lobanov, A. V. Novikov, and D. V. Yurasov, J. Surf. Invest.: X-Ray, Synchrotron Neutron Tech. **5**, 591 (2011).
5. M. N. Drozdov, Yu. N. Drozdov, A. V. Novikov, P. A. Yunin, and D. V. Yurasov, Semiconductors **48**, 1109 (2014).
6. F. Sanchez-Almazan, E. Napolitani, A. Carnera, et al., Appl. Surf. Sci. **231–232**, 704 (2004).
7. M. Junel and F. Laugier, Appl. Surf. Sci. **231–232**, 698 (2004).
8. M. N. Drozdov, Yu. N. Drozdov, N. D. Zakharov, D. N. Lobanov, A. V. Novikov, P. A. Yunin, and D. V. Yurasov, Tech. Phys. Lett. **40**, 601 (2014).
9. P. A. Yunin, Yu. N. Drozdov, M. N. Drozdov, A. V. Novikov, and D. V. Yurasov, Semiconductors **46**, 1481 (2012).

*Translated by O. Zhukova*